OPTICAL NAVIGATION PREPARATIONS FOR NEW HORIZONS PLUTO FLYBY[*]

William M. Owen, Jr.[(1)], **Philip J. Dumont**[(2)], **and Coralie D. Jackman**[(3)]

[(1)]*Jet Propulsion Laboratory, California Institute of Technology,*
4800 Oak Grove Drive 301–121, Pasadena CA 91109–8099, 818 354–2505, wmo@jpl.nasa.gov
[(2)]*KinetX, Inc., 21 W. Easy St., Simi Valley CA 93065, 805 520–8538, philip.dumont@kinetx.com*
[(3)] *KinetX, Inc., 21 W. Easy St., Simi Valley CA 93065, 805 520–8539,*
coralie.jackman@kinetx.com

Abstract: *The New Horizons spacecraft will encounter Pluto and its satellites in July 2015. As was the case for the Voyager encounters with Jupiter, Saturn, Uranus and Neptune, mission success will depend heavily on accurate spacecraft navigation, and accurate navigation will be impossible without the use of pictures of the Pluto system taken by the onboard cameras. We describe the preparations made by the New Horizons optical navigators: picture planning, image processing algorithms, software development and testing, and results from in-flight imaging.*

Keywords: *New Horizons, Pluto, navigation, optical navigation, image processing*

1. Introduction

Traditional optical navigation (Opnav) uses a spacecraft camera to take pictures of foreground target objects against a background of catalogued reference stars. This technique was pioneered in the 1960s [1] and enabled successful navigation of the six Voyager flybys of the outer planets [2] and Cassini's orbital operations at Saturn [3]. The New Horizons mission to Pluto will likewise use optical navigation: images will be acquired with the onboard science cameras and downlinked to Earth for processing.

Optical navigation does an excellent job of determining the inertial direction to the observed targets, but it does not do at all well at determining the distance to the targets, especially if their size and surface features are not well known. For a flyby encounter such as New Horizons at Pluto, approach imaging therefore determines the location of the incoming asymptote of the spacecraft's hyperbolic trajectory well, but it does little to improve the knowledge of the time of closest approach. Timing information becomes available only when the geometry has changed enough so that the spacecraft's incoming velocity vector makes a significant angle with the line of sight to the target. The last pictures are the most critical of all.

The New Horizons project has decided to mitigate navigation risks during the encounter period by using two navigation teams, a Project Navigation (PNAV) team at KinetX, Inc., and an Independent Navigation (INAV) team at the Jet Propulsion Laboratory.[†] Primary responsibility for spacecraft navigation rests with PNAV, including optical navigation picture planning and image processing, orbit determination (OD), and maneuver analysis. INAV serves as an

---

[†] Under a Memorandum of Understanding between JPL and KinetX, JPL Navigation is providing the optical navigation lead engineer to the PNAV team, reporting to the KinetX navigation team chief. Leveraging the nav experience of both organizations helps ensure a successful flyby.

independent check on PNAV's Opnav and OD results and provides technical direction to PNAV's optical navigators. The two teams use different software and different optical centerfinding techniques. We expect to compare results regularly and investigate any systematic differences that may arise during the course of the encounter.

2. Picture Planning

Picture planning is the process of determining how many optical navigation pictures to take, when to take them, where to point the cameras, and what camera parameters (exposure duration, and so forth) are to be used. Because optical navigation uses spacecraft resources, cooperation between the navigation team and the rest of the project (both engineers and scientists) is an essential aspect of the planning process. This is true for all projects, and it is particularly true for New Horizons owing to the spacecraft's limited downlink capability. The number of navigation pictures has a firm upper limit if all the pictures are to be received in a timely fashion, but navigation performance will suffer if there are not enough pictures. To produce the final picture schedule therefore requires negotiations and compromises, and the expected navigation performance in turn informs the design of the science plans.

As the operations teams prepare for the Pluto encounter, PNAV has developed a set of four optical navigation imaging campaigns (Table 1). The primary navigation camera is the Long-Range Reconnaissance Imager (LORRI) [4], and the backup camera is the Multi-spectral Visual Imaging Camera (MVIC), part of the Ralph instrument [5]. There are some MVIC images in the nominal plan, and for more critical loads, a contingency sequence will be built replacing all LORRI Opnavs with MVIC Opnavs. LORRI has two modes, 1x1 and 4x4 binning. Both are used in Opnav and serve different roles. LORRI 1x1 images have the best optical resolution, but exposure times are limited by pointing drift. In the 4x4 binned mode, the signal in 16 pixels is summed on the chip before readout, giving ¼ the resolution of the 1x1 mode with ¼ of the read noise. Relative control mode attitude enables much longer exposure times without smearing.

The first Opnav campaign is one week long and occurs July 20–27, 2014, one year before encounter. There will be two observations per day, with 5 LORRI 1x1 images per observation. The week-long campaign is designed to capture one full revolution of Charon. Nix and Hydra are expected not to be visible in these images.

The second campaign spans from January 25 to March 6, 2015. The first week of this campaign is like campaign 1, with 5 LORRI 1x1 images every 12 hours. As Nix and Hydra are expected to be visible in 4x4 LORRI images, we will take a set of 5 LORRI 4x4 images every 48 hours over the entire span of campaign 2. This campaign thus observes Pluto and Charon over one Charon revolution, this time at half the distance than campaign 1, and Nix & Hydra in 4x4 mode over one Hydra revolution.

As the targets get closer and become more resolved in Campaigns 3 and 4, Opnav plays a greater role in improving associated target body, barycenter and spacecraft uncertainties. The design of the near-encounter science planning utilizes the expected results from Opnav imaging to optimize the encounter sequences. Without Opnav, the *a priori* uncertainties in the spacecraft state, Pluto barycenter, and satellites ephemerides would require large mosaics to ensure the

target is somewhere in one of the images. With the addition of Opnav, the science operations team can optimize the encounter to ensure the largest science return.

Table 1. Summary of New Horizons Optical Navigation Imaging Campaigns

Campaign	Dates	Days from Pluto	LORRI 1x1	LORRI 4x4	MVIC Pan
1	7/20/14 — 7/27/14	−359 to −352	5 images/ 12 hours	None	None
2	1/25/15 — 2/1/15	−170 to −163	5 images/ 12 hours	5 images/ 48 hours	None
	2/1/15 — 3/6/15	−163 to −130	None	5 images/ 48 hours	None
3	4/5/15 — 4/15/15	−100 to −90	None	5 images/ 48 hours	None
	4/15/15 — 4/22/15	−90 to −83	4 images/ 12 hours	5 images/ 48 hours	2 images/ 24 hours
	4/22/15 — 4/15/15	−82 to −60	None	5 images/ 48 hours	None
4	5/28/15 — 6/23/15	−47 to −21	4 images/ 24 hours	6 images/ 24 hours	2 images/ 24 hours
	6/23/15 — 7/16/15	−21 to +1	5 images/ 24 hours	None	None

Campaign 3 spans April 5 through May 15, 2015. Over the entire campaign, the spacecraft will take a set of 5 LORRI 4x4 images every 48 hours. This is designed to further improve the ephemerides of the smaller satellites, Nix and Hydra. Additionally, the campaign contains the third week-long effort to improve uncertainties in the Pluto and Charon orbits. This campaign also contains the first instances of MVIC Pan-frame observations. These were added for contingency purposes, in the event LORRI fails at the start of this load and there is not enough turn-around time to sequence a backup load. Although the MVIC observations are not as extensive nor as accurate as LORRI, they provide a minimum dataset without breaking the data volume and thruster-count budgets.

There is a 15-day gap in Opnav imaging between Campaigns 3 and 4 when the spacecraft will enter spin mode to achieve higher downlink rates. This allows the flight team to clear the onboard data backlog before encounter.

Campaign 4 begins on May 28, 2015 (47 days before closest approach) and extends through July 16, 2015, one day after the encounter. The first 26 days will have daily observations with LORRI 1x1, 4x4, and MVIC pan-frame. At P − 21 days, only daily sets of LORRI 1x1 images will be taken. We expect to detect Nix and Hydra in the 1x1 exposures around this time, and so the 4x4 mode is no longer desirable. Additionally, there are no MVIC pictures in the nominal schedule after P − 21 days because contingency loads containing MVIC will be built for the remainder of the encounter in the event LORRI fails.

The current schedule contains 787 pictures beginning one year before encounter, including 330 LORRI pictures in its 4x4 binned mode and 32 MVIC pictures. Plans are in place to downlink quickly the most critical pictures, those taken immediately before the final orbit determination solution used to calculate maneuvers and those taken in the last week. Furthermore, the navigation team has identified some science pictures as dual use and will incorporate that imaging into the navigation data set.

3. Image Analysis Capabilities

The most difficult task faced by the optical navigators is that of extracting the (x, y) or (pixel, line) coordinates of images within the pictures. The brightness profile of the targets depends not only on the viewing geometry but also on the reflectance characteristics of the surface. Rigorous testing is required for any mission, but especially so when a priori knowledge is lacking. Pluto's radius remains uncertain to 10 km; the sizes of Nix and Hydra have not been measured directly but are only inferred from their brightness. Pluto is known to have significant albedo variations, and because it is in synchronous rotation with Charon's orbit, errors in Pluto's albedo map will translate directly into errors in its Charon-relative position and therefore into errors in Charon's eccentricity, in the mass ratio and in the location of the barycenter. This situation will improve as Pluto's apparent diameter grows during approach. The effects of Pluto's tenuous atmosphere on imaging are expected to be small. Likewise, errors in the size and assumed spherical shape of Nix and Hydra can be no larger than some fraction of their own radius.

For all these reasons it is important for optical navigators to have a variety of well tested algorithms at their disposal and to update their parameters (size, shape, albedo, even the choice of reflectance law) as the spacecraft nears its targets and our knowledge of them improves. These are the sorts of considerations which led the New Horizons project to maintain two navigation teams, and which (in part) led PNAV to develop its own Opnav capability without recourse to any existing INAV software.

3.1. PNAV Capabilities

Several unique aspects of the navigation problem from New Horizons have influenced the choice of algorithms and motivated the development of a high-fidelity image simulation capability. These include, but are not limited to, the long round trip light travel time to the spacecraft as it approaches the Pluto system, the low communication bandwidth and consequent limit on the number of Opnav images that will be shuttered, the spacecraft trajectory uncertainty, the Pluto system barycenter uncertainty (particularly along the Pluto–Sun vector), and the nature of the Pluto system environment, which has made the issue of hazard avoidance an urgent priority. The ability to simulate high fidelity images will help the project to mitigate the consequences of these uncertainties through a combination of Operation Readiness Tests (ORTs) and various what-if scenarios that present themselves from time to time. The simulation capability will be described in this section. The results obtained by exploiting this capability will be described in Section 4.

3.1.1. Architecture. The architecture of the PNAV OPNAV software has been strongly influenced by two choices made early in its development. MATLAB™ is the development

platform for the software. This decision was made because of MATLAB's extensive library of built-in image processing and optimization functions, as well its rich library of visualization tools. The MATLAB environment encourages the rapid prototyping of code with a minimum of coding errors. PNAV software uses the Navigation and Ancillary Information Facility's (NAIF) SPICE toolbox [6] to interrogate SPICE kernels produced by the project and by JPL. The information derived from these kernels includes spacecraft state and attitude in inertial space, the camera-to-inertial rotation matrix, conversion from UTC to ephemeris time (with leapseconds), and the planet and satellite ephemerides.

A model of the camera is required to generate simulated images. The camera is modeled as a system with two major components: the telescope and the detector. For our purposes, the aperture of the stop and the focal length of the telescope define the telescope. The detector is modeled by specifying the pixel size, the number of pixels, the quantum efficiency (QE) of the detector, the gain (electrons per Data Number [DN]), and the read noise. The physical size of the detector pixel and the telescope focal length define the footprint of the detector pixel (in radians) on the sky.

The New Horizons spacecraft has two cameras capable of shuttering Opnav images. The primary camera is the Long Range Reconnaissance Imager (LORRI) instrument [4]. LORRI has a diameter of 0.208 meter and a focal length of 2.619 meters. The detector is a 1024x1024 array with pixels that map to 5 microradians on the sky. The gain is 22 electrons per DN and the read noise is 22 electrons. The backup camera, in case LORRI fails, is the Multi-spectral Visible Imaging Camera (MVIC), which is part of the Ralph instrument [5]. MVIC has a stop diameter of 0.075 meter and a focal length of 0.653 meter. The detector has several filtered regions capable of time-delayed integration for use as a pushbroom camera, but Opnav will use an unfiltered 128x5024 array, used in stare mode, with a pixel size that maps to 20 microradians on the sky. The gain is 58.6 electrons per DN and the read noise is 30 electrons. One of us (WMO) calculated distortion models for both cameras, from observations of the star cluster M7 for LORRI and the star clusters M6 and M7 for MVIC. These models, which map position in the plane of the detector in a linear space into the distorted space of the camera, have been implemented in the PNAV Opnav software.

3.1.2. Image simulation. Image simulation requires the specification of the time (epoch) at which the image is shuttered. Given the epoch of the observation, the SPICE kernels return the inertial state and attitude of the spacecraft and the inertial positions of the target bodies (Pluto and its satellites) as viewed from the spacecraft. The spacecraft attitude and the rotation matrix from the camera reference frame to the space reference frame are combined to yield the rotation matrix **C** from inertial space to the camera frame.

With this information from the SPICE kernels, we can calculate the camera boresight in inertial space (right ascension and declination). Given the boresight and camera field of view (FOV), we can interrogate star catalogs to generate a list of stars which should be present in the image. Currently PNAV's software can access, from the MATLAB workspace, the Tycho-2, UCAC2, and UCAC4 star catalogs. The data returned for each candidate star include the inertial position at the observation epoch, corrected for proper motion, the magnitude of the star, and the stellar parallax if it is available. The software applies the correction for stellar aberration due to the

motion of the spacecraft and updates the parallax correction to the value it would have at the location of the spacecraft. The updated inertial positions are mapped to the camera coordinate system using the **C** matrix. The camera distortion model is applied to this location to predict the (pixel, line) location on the detector at which star will be imaged.

The photometry model assumes Vega as the standard candle. Hayes [7] has measured the flux from Vega arriving at the Earth as a function of wavelength. This flux, converted to photons, is integrated over the band pass appropriate for MVIC or LORRI. The number of detected photoelectrons from an object is determined by scaling the flux from Vega by the magnitude difference, the integration time of the exposure, the diameter of the stop, and the QE of the detector.

The Point Spread Function (PSF) of a camera is modeled as a two-dimensional Gaussian function. The parameterization of this non-rotationally symmetric model consists of two widths, characterized as standard deviations, for the two orthogonal directions, a rotation angle from the vertical axis of the detector, the amplitude of the function, and the (pixel, line) location of the center of the function. The PSF is normalized to an integrated value of one. For stars and unresolved target bodies, the normalized PSF is scaled to the integrated flux in detected photoelectrons derived from the photometry model.

The apparent inertial position of the geometric center of the target bodies relative to the spacecraft is calculated by the SPICE toolbox routine spkezr from the data in the spacecraft trajectory kernel, the planetary ephemeris kernel, and the satellite ephemeris kernel. This position is corrected for the aberration induced by the spacecraft velocity and for the light travel time from the target to the spacecraft, *i.e.*, the position returned is the "apparent" position from which the spacecraft receives light reflected from the position of the target at the time the light left it. This inertial position is mapped to the nonlinear (pixel, line) space on the detector using the camera to inertial rotation matrix and the camera distortion model.

For resolved target bodies, it is necessary to calculate the detected flux that is collected by each detector pixel that maps onto the surface of the body. Scaling the apparent magnitude as observed from the Earth to the apparent magnitude as seen from the spacecraft is necessary to calculate the total integrated flux from the body that is sensed by the detector. This flux is calculated by exercising the photometry model to calculate the total number of detected photoelectrons from the target. To determine the flux collected by each detector pixel, it is first necessary to determine which pixels map onto the surface of the body. Given the diameter of the target body, the spacecraft state vector, and the camera model, a straightforward analytic geometry calculation determines if a given detector pixel maps onto the body surface. For these pixels, the angle between the Sun–body vector and the local surface normal (incidence angle) and the angle between camera-to-surface intercept vector and the local surface normal (emission angle) are easily calculated. Given a uniform surface albedo, or in the case of Pluto a latitude- and longitude-dependent surface albedo derived from the albedo map derived by Buie et.al. [8] and a surface scattering law, the calculation of *I/F* for each pixel is straightforward. Currently, two surface scattering laws, Lambert and Lommel–Seeliger, have been implemented. Normalizing the resulting set of illuminated pixels to unity and scaling the resulting image to the

integrated detected photoelectrons yields the simulated image of the target body as sensed by the instrument.

Figure 1 shows an example of simulated LORRI image. This example image will be shuttered on July 9, 2015 04:29:00 UTC as part of Opnav campaign 4. The figure on the left is on a log stretch to bring up the stars in the image. The figure on the right is on a linear stretch. The locations of the green circles are the predicted positions of the stars in the image that have been returned from UCAC2 catalog. The slight discrepancy between positions of the simulated stars and the positions derived from the catalog is due primarily to the fact that the catalog positions have not had stellar aberration applied to them in the plot. Pluto and Charon are visible in the image. Note the evidence of albedo variations on the simulated image of Pluto.
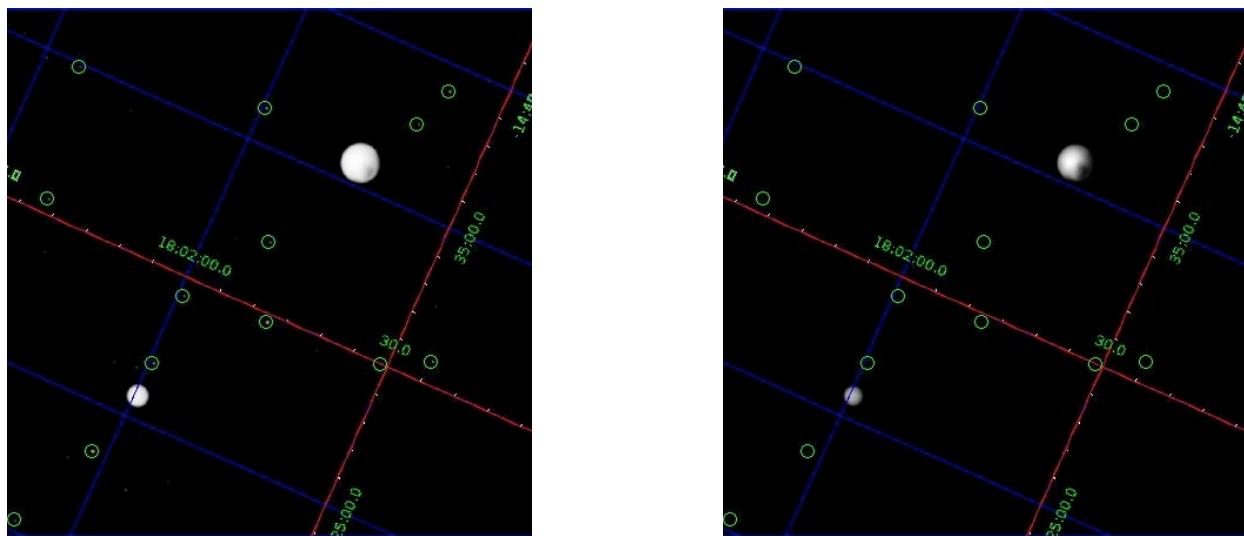

Figure 1. PNAV simulated LORRI images of Pluto, Charon and stars using a log stretch (left) and a linear stretch (right).

3.1.3. Image Analysis. The Opnav analysis products required from each image for the New Horizons OD include the predicted and measured target body geometric centers and the state partial derivatives, which are the partial derivatives of the target body geometric center with respect to the spacecraft state in inertial space relative to a reference target body. For New Horizons, the reference target body is Pluto.

The processing steps involved in the image analysis consist of estimating the geometric center of the catalog stars visible in the image, solving for the spacecraft attitude, and solving for the geometric center of the target bodies that are present in the image. Each of these steps is described in the following text.

3.1.4. Star Centerfinding. Given a spacecraft attitude kernel, we interrogate the star catalogs for a set of stars that are expected to be present in a picture. We map these star positions, corrected for stellar aberration and parallax, onto the image plane to obtain the *a priori* position for the stars. For each star in this set, the code isolates a small region in the image centered on the *a priori* position for the star. Several centerfinding algorithms have been implemented. A

matched-filter algorithm, using a well exposed image of a bright star as the basis for the filter, has proven useful for generating an initial guess for the center of the star. It has proven to be particularly robust in identifying faint stars in the presence of noise. A similar algorithm, which cross-correlates the subimage extracted from data with our canonical Gaussian PSF, is used to provide confirmation that the star is present in the subimage. This algorithm, however, does not appear to be as robust as the matched-filter algorithm in pulling a weak signal out of the noise.

PNAV's workhorse algorithm uses a nonlinear least squares estimator. The model function is our canonical Gaussian PSF. The estimated parameters include the amplitude, the two standard deviations, the rotation of the PSF, and most importantly, the (pixel, line) center of the star. We can also estimate the local background level. This estimator has proven robust against false positives and yields internally consistent results with a root mean square (rms) residual on the order of a tenth of a pixel (after repointing) to at least 11th magnitude stars for LORRI images with an exposure time of 0.1 second.

3.1.5. Spacecraft Attitude Solution. The attitude of the New Horizons spacecraft, derived from the SPICE attitude kernel, may be in error by as much as 40 pixels due to the nature of the spacecraft's attitude control system. In order to predict the locations of the target bodies in the image to the precision required by the OD filter, it is necessary to estimate the attitude of the spacecraft to less than one pixel. The PNAV Opnav software uses an estimator that solves for the spacecraft attitude that minimizes the residual, in a least-squares sense, between the measured and predicted positions of the stars in the image.

Three parameters are necessary to specify the spacecraft attitude. We have implemented an estimator that solves for two characterizations of these parameters. The first approach is image-plane based. It solves for the image plane shift, in two directions, and a rotation of the image that best registers the predicted star positions with their measured centers. The second algorithm is based directly on the spacecraft attitude, characterized by the **C** matrix. We use a nonlinear least squares estimator to solve for the three Euler angles of this matrix that minimize the residuals between the predicted and measured star locations. Figure 2 displays the result of a spacecraft repointing solution for an MVIC image of the asteroid 2002 JF56. The plot on the left shows the position residuals of the stars in the image as a function of magnitude before the repointing solution. The plot on the right shows the residuals after the repointing solution has been applied. Our working hypothesis for the ~one pixel residual in the *x* direction (the detector long axis), after repointing, is a problem with the MVIC distortion model calibration. Additional calibration campaigns are planned for 2013, 2014, and 2016.

3.1.6 Target Body Centerfinding. As the centerfinding algorithms employed for unresolved target bodies are the same as those for stars, this section describes only the techniques used to determine the centers of resolved objects. Two algorithms have been implemented. Both require a simulated image of the target body, as described in section 3.1.2. The code first isolates a region in the image (after the repointing solution) based on an *a priori* estimate of the target body center and size in pixels.

The first algorithm cross-correlates the model of the target with the data in the subarray to derive an estimate of the center. The second algorithm uses a nonlinear least squares estimator to find a

center solution that minimizes the difference between the model (the simulated image) and the data in the subarray in a least-squares sense. Simulations to date have shown that the two algorithms give comparable results. Because the least-squares algorithm is computationally intensive, we currently favor the cross-correlation algorithm.
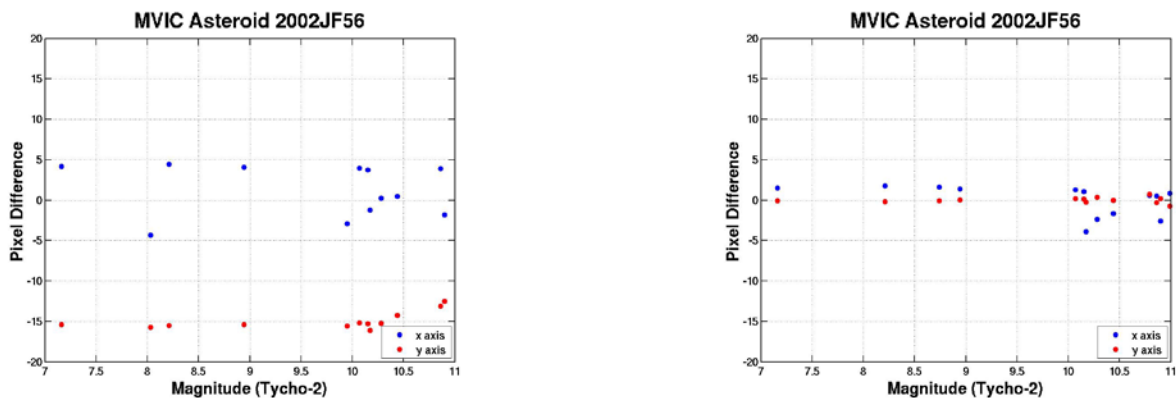

Figure 2. Prefit (left) and postfit (right) position residuals in pixel (blue) and line (red), plotted as a function of stellar magnitude, for a typical MVIC image. The repointing position produced a shift of (−2.69 pixels, +15.56 lines) and a rotation of −122.7 μrad about the boresight.

3.2. INAV Capabilities

INAV's optical navigation software [2, 9] is written primarily in Fortran, although the image display software and the picture I/O routines are in C. The software set has been used on NEAR [10] and Cassini [3], among others, and it can be used without modification for New Horizons as it is multimission by design.

3.2.1. Architecture. INAV's Opnav software comprises two subsystems. The Optical Navigation Image Processing System (ONIPS) extracts the (pixel, line) image centers from pictures. One of its two major programs can display a picture, with predicted image locations overlaid on it; the user can move the overlays either individually or as a group to make them match more closely the scene shown in the picture. For many missions this manual step provides the a priori image locations for the precision centerfinding routines, and we expect that New Horizons will use this technique too. The second major ONIPS program performs the precision centerfinding, described below in sections 3.2.3 to 3.2.6.

The second Opnav subsystem is the "Optical Navigation Program" set (ONP). Its components can predict image locations, produce plots, compute residuals, generate partial derivatives (analytically, not numerically), perform a camera pointing solution, and compute target error ellipses resulting from an OD solution. These functions have recently been incorporated into JPL's next-generation navigation tool, MONTE. However, the legacy ONP can still be used as a backup.

Typical processing first uses the ONP or MONTE to create a file containing predicted image locations for each picture to be analyzed. An analyst (sometimes with a second one watching) does the manual image registration; a crude pointing solution can be obtained here. Then ONIPS calculates the image centers. Next, ONP or MONTE performs a second pointing solution. The resulting file, in the same format as the original prediction file but with updated numbers, is merged into the previously delivered optical data for use by the OD team.

3.2.2. Image Simulation. The process of determining the predicted (pixel, line) locations of images within a picture follows the same steps as PNAV. The position and velocity of the camera are found, relative to the barycenter of the Solar System, by querying the appropriate ephemeris files and adding the results. (The camera need not be on a spacecraft; it can just as well be on a telescope in an observatory, and the software has seen extensive use in processing groundbased astrometry.) The position of each target body is likewise calculated, but at the "retarded time" when light left it. The calculation of the retarded time is done iteratively. The difference between these two position vectors—the target at the retarded time minus the camera at the observation time—yields the "true" position of the target. Finally, stellar aberration is applied by simply adding $\mathbf{v}/c$ to the unitized true position. The result is the "apparent" position.

Much the same process is used for stars, except that the star's position relative to the Solar System barycenter comes from a star catalog. The right ascension and declination have proper motion applied to the epoch of observation. If a star has a catalogued parallax, we have the distance to the star; if not, the distance is taken to be a very large number. Subtracting the spacecraft position, just as is done for nearby targets, automatically accounts for parallax.

INAV currently has no rigorous multimission picture generator *per se*. Some previous missions have had their own picture simulation software, often written in MATLAB. (An effort is currently underway to develop such a tool in the MONTE environment.) Instead, individual images, not entire pictures, are simulated as necessary as part of the centerfinding described next.

3.2.3. Image Analysis. The precision centerfinding tool in ONIPS can use a variety of techniques to determine the (pixel, line) location of the center of an image. All of them use a pixel array in which the camera bias and dark current background have been subtracted. The DN values have uncertainties attached to them, comprising shot noise and read noise added in quadrature; ONIPS uses extremely large uncertainties to indicate bad or missing pixels.

3.2.4. Star Centerfinding. The usual algorithm for finding centers of stars and very small targets is a two-dimensional circular Gaussian fit. Solution parameters include the (x, y) coordinates of the center, the height of the image, and the background. Once this solution converges, the width of the Gaussian is added to the parameter set and the process is repeated. Experience has shown that a circularly symmetric Gaussian usually produces reliable centers, even if the camera PSF is decidedly not Gaussian. The symmetry of the fitting function ensures that any mismatch to the PSF will likely produce symmetrical DN residuals, and any remaining asymmetry can often be absorbed in the camera distortion model. Nevertheless, ONIPS can also use an elliptical Gaussian, although not at an arbitrary position angle.

Another method, used routinely for Voyager [2] and occasionally since then, is applied when the camera attitude changes during an exposure, resulting in trailed star images. Here the PSF is modeled as a Lorentz function, $h/(1+(r/a)^2)$, where h is the image height, r is the distance from the center of the image and a is the half width at half maximum. This function is convolved with a line segment representing the image smear to construct the simulated image. The solution is performed using two levels of least-squares iterations: one level for the parameters for each star, a second level for the length and position angle of the smear vector, taken as constant for all star images. The relatively short exposures used by modern CCD cameras are expected to render this technique unnecessary for New Horizons.

3.2.5. Spacecraft Attitude Solution. INAV's Opnav tools care only about the camera attitude, not the attitude of the spacecraft itself. It is traditional to obtain the predicted camera attitude from each picture's header records, assuming that the picture file generation process has access to the as-flown (telemetry) attitude. We expect this to be the case for New Horizons. If the telemetered attitude is not available, the planned attitude can be used instead. Standard practice is to solve for three rotations about the principal axes of the camera and then use these angles to update the **C** matrix. The ONP can also solve for the right ascension and declination of the boresight, along with a twist angle, but the R.A. and twist angles become highly correlated when the camera is pointed near one of the celestial poles.

3.2.6. Target Body Centerfinding. INAV's primary algorithm for resolved bodies is limb scanning. The software establishes some number of radial scans, each emanating from the presumed center of the image at a different position angle. The DN array is interpolated at one-pixel intervals along each scan line to give a linear array of observed values. At each of these points, the angles of incidence and emission are computed (if the point is on the surface), and a reflectance law yields the computed brightness at that point. This process yields another linear array, this one containing predicted values. The two arrays are correlated, and the location of the correlation peak provides the coordinates of the observed limb along that scan line. Once all the limb points have been thus found, a least-squares solution determines the center of the image. Terminator scans can also be used, but as the transition from light to shadow is much more gradual than the transition from lit surface to dark space, terminator scans generally carry a much lower weight.

Limb scanning works best if one has good knowledge of the size and shape of the target body. It is easy to see that if one has an incorrect value for the radius of a spherical body, the center from limb scanning may be biased along the sun line. Biases can also result if the reflectance law is inappropriate or has wrong parameters, or if the assumed point-spread function (convolved with the predicted brightness array) is incorrect. The INAV Opnav team plans to keep careful watch over the limb scan results, solving for the sizes and shapes of the targets, and examining carefully the reflectance laws.

A whole-body cross-correlation is also available. This technique may prove useful in that awkward regime in which the body's apparent diameter is too large to use point-source techniques and too small to use limb fitting reliably.

4. Image Analysis Results

Inflight imaging has mostly been limited to testing and periodic camera calibrations, with the notable exception of an intensive imaging campaign during New Horizon's 2007 gravity assist at Jupiter. The PNAV and INAV optical navigators have analyzed many of the calibration images and some of the Jupiter dataset, especially images of Jupiter's smaller satellites. This section describes our results.

4.1. Geometric Calibration

The New Horizons science instruments have been calibrated repeatedly since August 2006. Opnav is interested primarily in geometric calibration, to determine the departure of the optics from the ideal "gnomonic" projection. (Instead of performing a rigorous photometric calibration, we simply determine the catalogued magnitude at which star residuals degrade significantly.)

For LORRI we can use a five-parameter model [9] which accounts for camera focal length, cubic radial distortion in the optics, and tip/tilt terms in x and y. Pixels can be modeled as parallelograms, but as there is no significant evidence that the pixels are not in fact square, a simpler model appears below. Given a vector $\mathbf{P}$ expressed in camera coordinates ($+x$ to the right, $+y$ down, $+z$ toward the sky) and the camera focal length f, we use the gnomonic projection to map the vector into an ideal (ξ, η) position in the focal plane:

$$\xi = P_1\,(f/P_3), \quad \eta = P_2\,(f/P_3).$$

We then incorporate the effects of distortion and tip/tilt:

$$\Delta\xi = \varepsilon_2\xi(\xi^2 + \eta^2) + \varepsilon_5\xi\eta + \varepsilon_6\xi^2, \quad \Delta\eta = \varepsilon_2\eta(\xi^2 + \eta^2) + \varepsilon_5\eta^2 + \varepsilon_6\xi\eta.$$

Finally, the corrected positions are transformed into (pixel, line) coordinates:

$$p = p_0 + (\xi + \Delta\xi)/s, \quad l = l_0 + (\eta + \Delta\eta)/s.$$

There is a significant pincushion distortion (ε_2), amounting to 1.73 ± 0.01 pixels in the corners of the field, and less pronounced (but still significant) tip and tilt of the detector relative to the optical focal plane. The parameters obtained from the 2006 calibration (Table 2) are still used, as subsequent calibrations have produced results which agree well with them.

The simple model used for LORRI is not accurate enough for MVIC's long, skinny field. The MVIC calibration model uses instead a set of Legendre polynomials, up to fifth order, to account for departures from gnomonic projection. Calibration results to date have suffered because the selected target (open clusters M6 and M7) has relatively few stars between the clusters. Some parts of the detector have not been adequately sampled as a result. Future calibrations, beginning in summer 2013, will also image the "Wishing Well Cluster" NGC 3532 and the rich star field surrounding it. We expect to get better calibration results for both cameras from this target.

Table 2. LORRI camera parameters.

Parameter	Value
Camera focal length, f	2619.008 ± 0.021 mm
Pixel linear dimension, s	0.013 mm (assumed)
Coordinates of optical axis, (p_0, l_0)	(512.5, 512.5) (assumed)
Cubic radial distortion coefficient, ε_2	$(+2.696 \pm 0.016) \times 10^{-5}$ mm^{-2}
Tip/tilt coefficient in x, ε_5	$(+1.988 \pm 0.091) \times 10^{-5}$ mm^{-1}
Tip/tilt coefficient in y, ε_6	$(-2.864 \pm 0.099) \times 10^{-5}$ mm^{-1}

4.2. Jupiter Flyby Imaging

When the New Horizons spacecraft flew by Jupiter in late February and early March 2007, the LORRI camera took a series of exposures of two of Jupiter's minor outer satellites, Himalia and Callirrhoe. A subset of the images of each of these satellites was processed with the PNAV Opnav software. The two main reasons for processing these images were to establish that the software could centerfind on real objects and to compare results with INAV.

Images of Himalia were taken with exposure times of 0.04, 0.1, and 1.0 second. We processed the 0.1 and 1.0 second images. The 0.04 second images, because of the short exposure time, did not have an adequate number of stars in the FOV to do a repointing solution. The 1.0 second exposures had a significant image smear due to attitude motion within the attitude control dead band. The engineering level images were processed. This tested our code's ability to subtract the mean and bias field backgrounds and flat field the images. The matched filter algorithm was used for centerfinding on both stars and target bodies for the 0.1 second exposures. The nonlinear least-squares algorithm was used for the 1.0 second images because of the large image smear. Stars as faint as magnitude 12.7 were successfully processed in the 0.1 second exposures.

Five images of Callirrhoe were processed. These images were taken in the LORRI 4x4 mode. The first four images had an integration time of 10 seconds and the fifth image had an integration time of 5 seconds. With a diameter of eight kilometers, Callirrhoe is unresolved in all of the images. Because of the relatively long integration time and the improved signal-to-noise ratio in the LORRI 4x4 mode, we are able to detect stars as faint as fifteenth magnitude in these images. The repointing solution, however, was limited to stars brighter than thirteenth magnitude.

Figure 3 presents real and simulated images of Himalia and Callirrhoe. In each case the real image appears on the left, the corresponding simulated image on the right. The residual in right ascension and declination are shown for Himalia. The Callirrhoe diagram instead displays the predictions and measurements in (pixel, line) for both PNAV and INAV. Insignificant differences of a few hundredths of a pixel are evident.
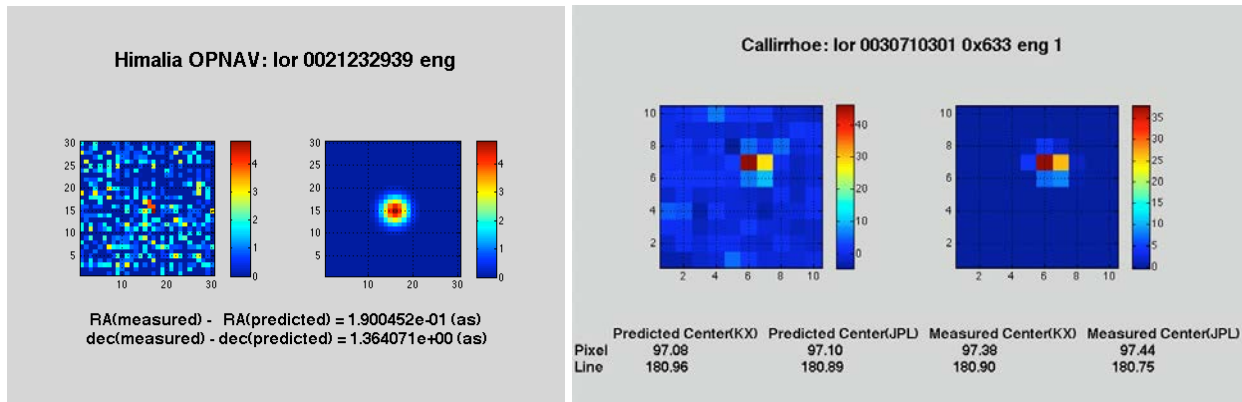
Figure 3. Comparison of real and simulated images of Himalia (left) and Callirrhoe (right) at their estimated (pixel, line) center.

5. Conclusions

Each of the two New Horizons navigation teams—Project Navigation at KinetX, Inc., and Independent Navigation at JPL—has its own optical navigation system, capable of predicting image locations within a picture, analyzing imaging data to locate the observed centers of images, forming residuals (observed minus computed) for these observations, and calculating the necessary partial derivatives of the image centers with respect to the various parameters used in the orbit determination process. The teams have compared their results for the Jupiter dataset and found satisfactory agreement. We have laid out an Opnav imaging plan for 2015 which captures enough data to meet navigation accuracy requirements and which is reasonably robust against the possible loss of our preferred camera.

We believe that both PNAV and INAV optical navigation teams are ready to support the New Horizons encounter with the Pluto system.

6. Acknowledgments

7. References

[1] Owen, W. M. Jr., Duxbury, T. C., Acton, C. H. Jr., Synnott, S. P., Riedel, J. E., and Bhaskaran, S. "A Brief History of Optical Navigation at JPL." 31st Annual AAS Guidance and Control Conference. Breckenridge, CO, USA, 2008.

[2] Riedel, J. E., Owen, W. M. Jr., Stuve, J. A., Synnott, A. P., and Vaughan, R. AM. "Optical Navigation During the Voyager Neptune Encounter." AIAA/AAS Astrodynamics Conference. Portland, OR, USA, 1990.

[3] Gillam, S. D., Owen, W. M. Jr., Vaughan, A. T., Wang, T.-C. M., Costello, J. D., Jacobson, R. A., Bluhm, D., Pojman, J. L., and Ionasescu, R. "Optical Navigation for the Cassini/Huygens Mission." AIAA/AAS Astrodynamics Specialist Conference. Mackinac Island, MI, USA, 2007.

[4] Cheng, A. F., Weaver, H. A., Conard, S. J., Morgan, M. F., Barnouin-Jha, O., Boldt, J. D., Cooper, K. A., Darlington, E. H., Grey, M. P., Hayes, J. R., Kosakowski, K. E., Magee, T., Rossano, E. R., Sampath, D., Schlemm, C., and Taylor, H. W., "Long Range Reconnaissance Imager on New Horizons." Space Science Reviews, Vol. 140, No. 1–4, pp. 189–215, 2008.

[5] Reuter, D. C., Stern, S. A., Scherrer, J., Jennings, D. E., Baer, J., Hanley, J., Hardaway, L., Lunsford, A., McMuldroch, S., Moore, J., Olkin, C., Parizek, R., Reitsema, H., Sabatke, D., Spencer, J., Stone, J., Throop, H., Van Cleve, J., Weigle, G. E., and Young, L. A. "Ralph: A Visible/Infrared Imager for the New Horizons Pluto/Kuiper Belt Mission." Space Science Reviews, Vol. 140, No. 1–4, pp. 129–154, 2008.

[6] Acton, C., Bachman, N., Diaz Del Rio, J., Semenov, B., Wright, E., and Yamamoto, Y. "SPICE: A Means for Determining Observation Geometry." EPSC–DPS Joint Meeting 2011. Nantes, France, 2011.

[7] Hayes, D. S. "An Absolute Spectrophotometric Calibration of the Energy Distribution of Twelve Standard Stars." Astrophysical Journal, Vol. 159, pp. 165–176, 1970.

[8] Buie, M. W., Grundy, W. M., Young, E. F., Young, L. A., and Stern, S. A. "Pluto and Charon with the Hubble Space Telescope. II. Resolving Changes on Pluto's Surface and a Map for Charon." Astronomical Journal, Vol. 139, pp. 1128–1143, 2010.

[9] Owen, W. M. Jr., "Methods of Optical Navigation." 21st AAS/AIAA Space Flight Mechanics Meeting. New Orleans, LA, USA, 2011.

[10] Owen, W. M. Jr., Wang, T.-C., Harch, A., Bell, M., and Peterson, C. "NEAR Optical Navigation at Eros." AAS/AIAA Astrodynamics Specialists Conference. Quebec City, Quebec, Canada, 2001.